Arch Toxicol (2011) 85:743–750
DOI 10.1007/s00204-010-0545-5

INORGANIC COMPOUNDS

Cytotoxicity and genotoxicity of silver nanoparticles in the human lung cancer cell line, A549

Rasmus Foldbjerg · Duy Anh Dang · Herman Autrup

Received: 9 December 2009 / Accepted: 15 April 2010 / Published online: 29 April 2010

Abstract Nanomaterials, especially silver nanoparticles (Ag NPs), are used in a rapidly increasing number of commercial products. Accordingly, the hazards associated with human exposure to nanomaterials should be investigated to facilitate the risk assessment process. A potential route of exposure to NPs is through the respiratory system. In the present study, we investigated the effects of well-characterized PVP-coated Ag NPs and silver ions (Ag+) in the human, alveolar cell line, A549. Dose-dependent cellular toxicity caused by Ag NPs and Ag+ was demonstrated by the MTT and annexin V/propidium iodide assays, and evidence of Ag NP uptake could be measured indirectly by atomic absorption spectroscopy and flow cytometry. The cytotoxicity of both silver compounds was greatly decreased by pretreatment with the antioxidant, *N*-acetyl-cysteine, and a strong correlation between the levels of reactive oxygen species (ROS) and mitochondrial damage ($r_s = -0.8810$; $p = 0.0039$) or early apoptosis ($r_s = 0.8857$; $p = 0.0188$) was observed. DNA damage induced by ROS was detected as an increase in bulky DNA adducts by ^{32}P postlabeling after Ag NP exposure. The level of bulky DNA adducts was strongly correlated with the cellular ROS levels ($r_s = 0.8810$, $p = 0.0039$) and could be inhibited by antioxidant pretreatment, suggesting Ag NPs as a mediator of ROS-induced genotoxicity.

Keywords Silver · Nanoparticles · Reactive oxygen species · Apoptosis · Bulky DNA adducts

R. Foldbjerg (✉) · D. A. Dang · H. Autrup
Nanoparticle Safety Group,
Department of Environmental and Occupational Medicine,
Institute of Public Health, Aarhus University,
Bartholins Allé 2, Building 1260, 8000 Aarhus, Denmark
e-mail: rfol@mil.au.dk

Introduction

The rapid expansion of nanotechnology has led to a large increase in the number of products containing nano-sized materials. However, the novel physicochemical properties of materials on the nanoscale emphasize the need for proper assessment of the potential effects to human health. Specific concern is expressed about the possible toxicity of nanoparticles (NPs) defined as particles having at least two dimensions below 100 nm. Although evidence suggests that NPs could have adverse effects on human health (Xia et al. 2009), the fundamental cause/effect relationships are not yet fully understood.

Currently, silver (Ag) is by far the most commercialized nano-compound according to the Woodrow–Wilson database on nano-products (www.nanotechproject.org). Monovalent silver compounds have been used extensively for antimicrobial treatment and prophylaxis for decades, and recent studies suggest that the antimicrobial activity is retained in Ag NPs (Ip et al. 2006; Melaiye et al. 2005). This has led to the use of Ag NPs in a variety of consumer products including electronics, cosmetics, household appliances, textiles and food production as well as in medical products (Wijnhoven et al. 2009).

Previous studies have reported membrane leakage, decreased viability and inhibition of mitochondrial activity upon Ag NP exposure in different cell lines, e.g., BRL4A rat liver cells (Hussain et al. 2005), PC-12 neuroendocrine cells (Hussain et al. 2006), germline stem cells (Braydich-Stolle et al. 2005) and rat alveolar macrophages (Carlson et al. 2008). It has been proposed that the induction of reactive oxygen species (ROS) is a general mechanism of NP-mediated cytotoxicity which is supported by studies showing that in vitro exposure to Ag NPs cause reduction in GSH, elevated ROS levels, lipid peroxidation and

increased expression of ROS responsive genes (Arora et al. 2008; Carlson et al. 2008; Kim et al. 2009). Furthermore, an Ag NP-mediated increase in ROS was associated with DNA damage, apoptosis and necrosis (Arora et al. 2008; Foldbjerg et al. 2009; Kim et al. 2009).

In the present study, we investigated the uptake and cytotoxic effects of well-characterized Ag NPs in the human lung carcinoma cell line, A549. Our results suggest that Ag NPs are taken up by the cells leading to increased production of ROS and ultimately apoptotic and necrotic cell death. Antioxidant treatment could reduce the production of ROS and greatly increase cell viability. Furthermore, formation of bulky DNA adducts could be prevented by antioxidant treatment, suggesting that ROS formation may be a key event in Ag NP toxicity.

Materials and methods

Materials and reagents

Silver nanoparticle powder coated with 0.2% PVP (poly vinyl pyrrolidone) was obtained from NanoAmor (Houston, USA). According to the manufacturer, the Ag NPs are spherical and 30–50 nm in size. The purity was measured by the manufacturer using inductively coupled plasma spectrometry (ICP), and metal contaminants in the Ag NP powder were reported to be below 0.1% (Al, 10 ppm; As < 0.5 ppm; Bi, 20 ppm; Cu, 17 ppm; Fe, 56 ppm; Ni, 3 ppm; Pb, 9 ppm; Sb < 0.5 ppm; Si, 41 ppm). $AgNO_3$ (dissolved in dH_2O, 0.1 M) was obtained from Sigma–Aldrich. DMEM medium (#61965), heat-inactivated fetal bovine serum (FBS) (Gibco, #10500-064), L-Alanyl-L-Glutamine, annexin V-FITC, propidium iodide (PI), penicillin and streptomycin were purchased from Invitrogen. HNO_3 (69%), 2′,7′-dichlorodihydrofluorescein diacetate (H_2DCF-DA), 3-(4,5-dimethyl-2-thiazolyl)-2,5-diphenyl-2H-tetrazolium bromide (MTT), fluorescamine, *N*-acetyl-L-cysteine (NAC), dimethylsulfoxide (DMSO), acetonitril, HEPES, NaCl, $CaCl_2$ and phosphate-buffered saline (PBS) were purchased from Sigma–Aldrich. 5× lysis buffer (#1897675) was obtained from Roche.

Ag NP stock solution

The Ag NP solution was prepared in ddH_2O by sonication, centrifugation and filtration as described previously (Foldbjerg et al. 2009). The concentration of the Ag NP stock solution was determined by dissolving the NP suspension in 69% HNO_3 followed by atomic absorption spectroscopy (AAS) on a Perkin–Elmer AAnalyst 300 AAS (Perkin–Elmer, DK) mounted with a silver lumina hollow cathode lamp (Perkin–Elmer, DK). Duplicate measurements were taken within the linear detection range of the AAS (silver detection limit was 36 µg/l). The endotoxin level of the Ag NP stock solution was measured by the Limulus amebocyte lysate (LAL) test (QCL-1000, Lonza) according to the manufacturer's instructions. Final Ag NP dilutions contained below one endotoxin units per ml at the highest Ag NP dose.

Ag NP characterization

The Ag NPs were previously characterized by Foldbjerg et al. (2009), and the main characteristics are summarized in Table 1.

Cell culture

The A549 human lung carcinoma epithelial-like cell line was obtained from ATCC (#CCL-185). Cells were cultured in DMEM supplemented with L-alanyl–L-glutamine (2 mM), penicillin (100 µg/ml), streptomycin (100 U/ml) and 10% heat-inactivated FBS. Cells were maintained in a humidified atmosphere at 37°C and 5% CO_2.

Exposure protocol

Exposure was initiated at 100% confluence, and all assays were done in DMEM medium containing antibiotics and 1%

Table 1 Ag NP characterization (Foldbjerg et al. 2009)

Condition	Method	Result
Ag NP powder	Powder X-ray diffraction (PW-XRD)	Approximately 78.1 nm
Stock solution (MilliQ)	TEM	69 ± 3 nm (SE) Spherical, multi-facetted or slightly elongated shapes
Stock solution (MilliQ)	DLS	121 ± 6 nm (SD) ζ-potential = −21.8 mV
RPMI 1640 media + 1% FBS	DLS (24 h at 37°C)	149 ± 37 nm (SD) ζ-potential = −11.6 mV

FBS. The dose of $AgNO_3$ was calculated based on silver mass and expressed as Ag+. Doses ranged from 0 to 20 μg/ml Ag NPs and 0 to 10 μg/ml Ag+. Antioxidant treatment by NAC (10 mM, 1 h) was done prior to Ag exposure.

Atomic absorption spectroscopy (AAS) assay

At the end of Ag NP exposure, cells were washed twice in PBS, trypsinized, spun down and resuspended in nitric acid (69%). Cells were lysed at room temperature by sonication for 15 min in a water bath and allowed to digest for 1 h. Finally, samples were centrifuged at 5,000×*g* for 2 min to eliminate debris. Supernatants were diluted to a final concentration of 5% HNO_3 and AAS was performed as described above.

Side scatter measurements

After Ag NP exposure, cells were trypsinized, centrifuged and resuspended in PBS. The light side scatter intensity was measured by flow cytometry (Quanta SC MPL, Beckman Coulter). Cellular debris was gated out, and the mean side scatter was recorded by the Quanta SC MPL Analysis software based on 20,000 events.

MTT assay

The MTT assay was used to measure mitochondrial activity as previously described but with minor modifications (Mosmann 1983). Following exposure, cell culture medium was discarded, and cells were incubated with 100 μl of MTT solution (0.5 mg/ml dissolved in DMEM without FBS) for 2 h at 37°C, 5% CO_2. The MTT solution was then discarded, and 100 μl of DMSO was added to each well. Optical density was read on a microplate reader at 550 nm, with a reference at 655 nm (EL800, Bio-Tek Instruments, Inc.). Viability was calculated as the ratio of the mean of OD obtained for each condition to that of the control (no particle) condition.

ROS assay

To measure the intracellular generation of reactive oxygen species (ROS), the fluorescent marker H_2DCF-DA was used as previously described but with modifications (Foldbjerg et al. 2009). Cells were grown in 96-well plates until confluency. Prior to Ag NP exposure, cells were loaded with 50 μM H_2DCF-DA in PBS for 20 min and washed once in PBS. Subsequently, the cells were exposed to Ag NPs for 24 h. After exposure, cells were washed once in PBS, and 100 μl PBS was added to each well. Fluorescence intensity was detected at Ex/Em = 485/535 nm on a Wallac Victor^2 Multilabel Counter (Perkin–Elmer). The ability of Ag NPs to react with the H2DCF probe in an acellular environment was tested and found to be negative. For standardization purposes, the protein content in each well was subsequently measured by fluorescamine. The non-fluorescent compound, fluorescamine, reacts rapidly with primary amines in proteins to form highly fluorescent moieties that can be detected as described previously (Lorenzen and Kennedy 1993). In brief, 50 μl 1× lysis buffer was added to each well followed by addition of 50 μl fluorescamine dissolved in acetonitril (0.5 mg/ml). The fluorescence intensity was detected at Ex/Em = 355/460 nm using a Wallac Victor^2 Multilabel Counter. ROS measurements were normalized to the amount of protein, and the normalized numbers were used to calculate the increase in ROS compared to untreated controls.

Annexin V/PI assay

Cells positive of apoptosis and necrosis were measured by the annexin V/propidium iodide (PI) assay (van Engeland et al. 1996). The externalization of phosphatidylserine as a marker of early-stage apoptosis was detected by the annexin V protein conjugated to FITC, whereas membrane damage due to late-stage apoptosis/necrosis was detected by the binding of PI to nuclear DNA. After NP exposure, cells were collected, washed in binding buffer (10 mM HEPES, pH 7.4; 140 mM NaCl; 2.5 mM $CaCl_2$) and incubated in the dark for 10 min at room temperature in 100 μl binding buffer containing Annexin V-FITC (40 μl/ml) and PI (1 μg/ml). After incubation, 400 μl binding buffer was added to each sample, and cells were kept on ice. The 488-nm laser was used for excitation, and FITC was detected in FL-1 by a 525/30 BP filter, while PI was detected in FL-2 by a 575/30 BP filter. Standard compensation was done in the Quanta SC MPL Analysis software (Beckman Coulter) using single-stained and unstained cells. For each sample, 20,000 cells were analyzed and apoptotic (Annexin V+, PI−), necrotic (Annexin V+, PI+) and live (Annexin V−, PI−) cells were expressed as percentages of the 20,000 cells.

DNA adducts (^{32}P postlabeling)

After exposure, cells were harvested, DNA was isolated, and DNA adducts were determined by the butanol enrichment procedure as previously described (Bak et al. 2006; Nielsen et al. 1996). The adduct spots were measured by phosphorimage analysis (Molecular Image, Bio-Rad GS-363). The BaP-diolepoxide DNA adduct was included in the analysis as an internal standard. The level of DNA adducts was obtained as the average of three independent assays and expressed as adducts per 10^8 nucleotides (n/10^8 nt). The limit of detection was 0.1 n/10^8 nt.

Statistical evaluation

The data were expressed as mean ± standard deviation (SD) of at least three independent experiments. Data were subjected to statistical analysis by Student's *t*-test to test the difference between treatment ± NAC at each silver dose. When appropriate, the difference between silver-treated samples and the untreated control was tested by one-way analysis of variance (ANOVA) followed by Dunnet's test. Spearman's rank correlation coefficient (r_s) was calculated to test the association between ROS and different variables. A value of $p < 0.05$ was considered significant. Excel 2007 and Sigma Plot for Windows version 11 were used for statistical analysis.

Results

Ag NP uptake

It has been proposed that the intracellular concentration of NPs is reflected in the intensity of light side scatter measured by flow cytometry (Suzuki et al. 2007). Using this experimental approach, a dose-dependent increase in cellular uptake of Ag NPs was detected at doses from 5 to 15 µg/ml after 24-h NP exposure (Fig. 1a). A similar dose-dependent increase in side scatter was detected when the cells had been pretreated by NAC for 1 h, suggesting that the increased cellular granularity is not an artifact caused by dying cells (NAC reduces cell death as described in Fig. 2).

To further verify the uptake of silver in A549 cells at different time points and doses, AAS analyses were employed (Fig. 1b). Silver could not be detected in controls and cells exposed to Ag NP for 1 min. However, at 4 and 24 h, a dose- and time-dependent accumulation of silver could be measured in A549 cell lysates.

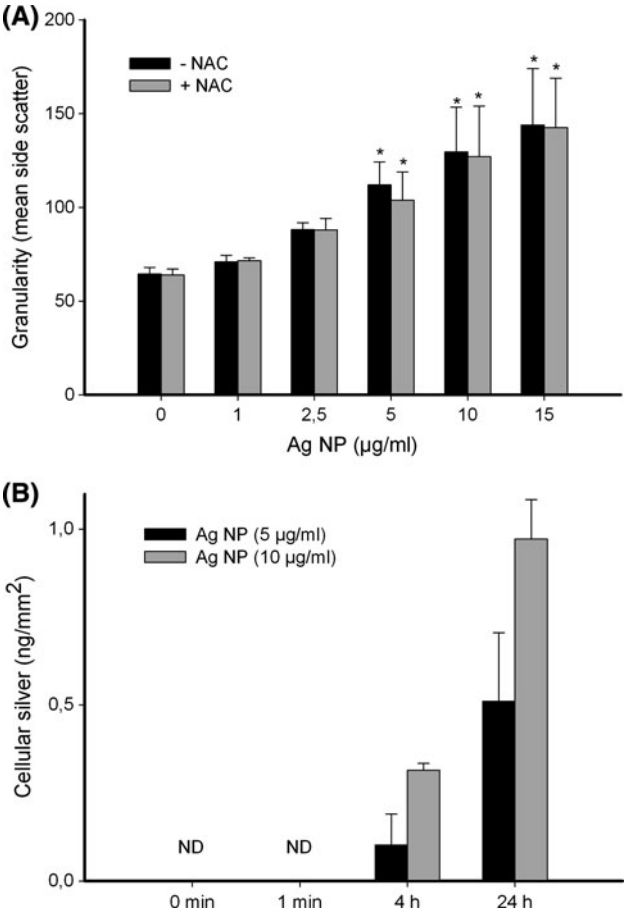

Fig. 1 Ag NP uptake. **a** Cells were pretreated for 1 h in media ± NAC (10 mM) and exposed to different concentrations of Ag NPs for 24 h. After exposure, the cells were assayed for light side scatter intensity by flow cytometry. **b** Cells were treated with Ag NPs at different time points, and the silver concentration of cell lysates was determined by AAS. The data are expressed as mean ± SD of three independent experiments. *Asterisks* denote significant ($p < 0.05$) difference from the untreated control. ND = not detectable

Cytotoxicity

The toxicity of Ag NP and Ag+ was assessed by the decrease in mitochondrial activity using the MTT assay (Fig. 2). A reduction in mitochondrial function of A549 cells exposed to Ag NPs for 24 h was observed in a dose-dependent manner (0–20 µg/ml) (Fig. 2a). Ag+ revealed similar toxic effects on mitochondrial function compared to Ag NPs although at lower doses (0–10 g/ml) (Fig. 2b). The toxicity of both Ag NPs and Ag+ could be significantly reduced by pretreating the cells for 1 h with high doses of the antioxidant, NAC (10 mM) (Fig. 2).

The annexin V/PI assay was used to investigate the mechanism of cell death induced by Ag NP exposure for 24 h (Fig. 3). The dose-dependent effect of Ag NPs on cell viability (Fig. 3a) was similar to that detected by the MTT assay, and this effect was partly prevented by NAC pretreatment. Cell death was primarily due to a dose-dependent increase in necrosis/late apoptosis at 2.5–15 µg/ml Ag NPs (Fig. 3c), whereas only a minor increase in early apoptosis was detected (Fig. 3b).

ROS

The H_2DCF-DA assay was used to assess the impact of Ag NP and Ag+ exposure on the cellular ROS production (Fig. 4). After 24-h exposure, Ag NP concentrations ranging from 2.5 to 15 µg/ml induced significant ROS (Fig. 4a). When cells were treated with NAC (10 mM) for 1 h before Ag NP exposure, the ROS levels were significantly reduced. Ag+ doses from 2 to 10 µg/ml also induced significant ROS which was reduced by NAC pretreatment (Fig. 4b). Generally, the Ag NPs induced higher increases in ROS than Ag+, suggesting that ROS, caused by Ag NPs, are not solely due to the potential release of Ag+.

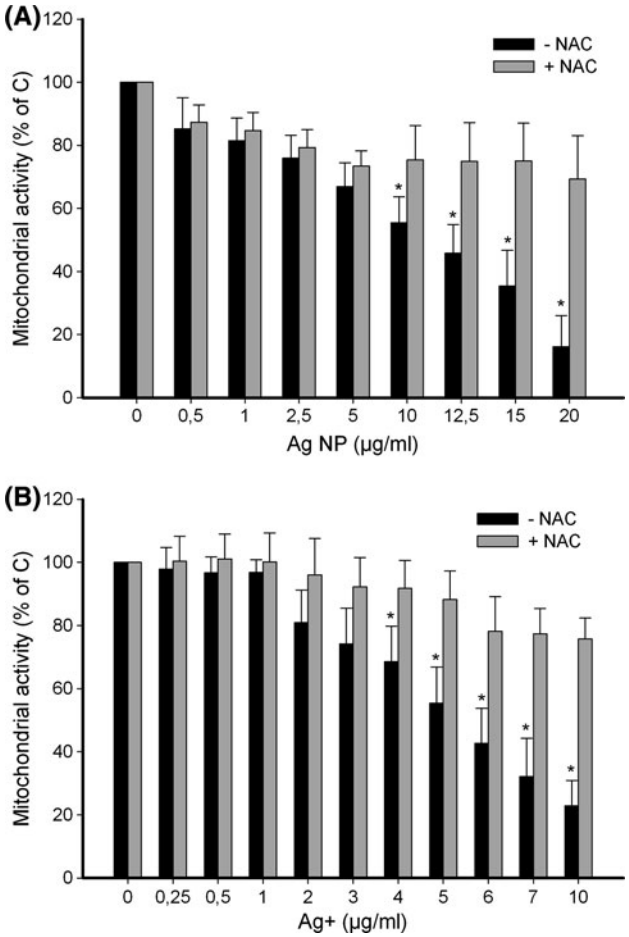

Fig. 2 Effect of Ag NPs and Ag+ on mitochondrial activity. Cells were pretreated for 1 h in media ± NAC (10 mM), exposed to different concentrations of **a** Ag NPs or **b** Ag+ for 24 h, and mitochondrial activity was measured by MTT. The data are expressed as mean ± SD of three independent experiments. *Asterisks* denote significant ($p < 0.05$) difference between samples ± NAC treatment at each Ag NP or Ag+ dose

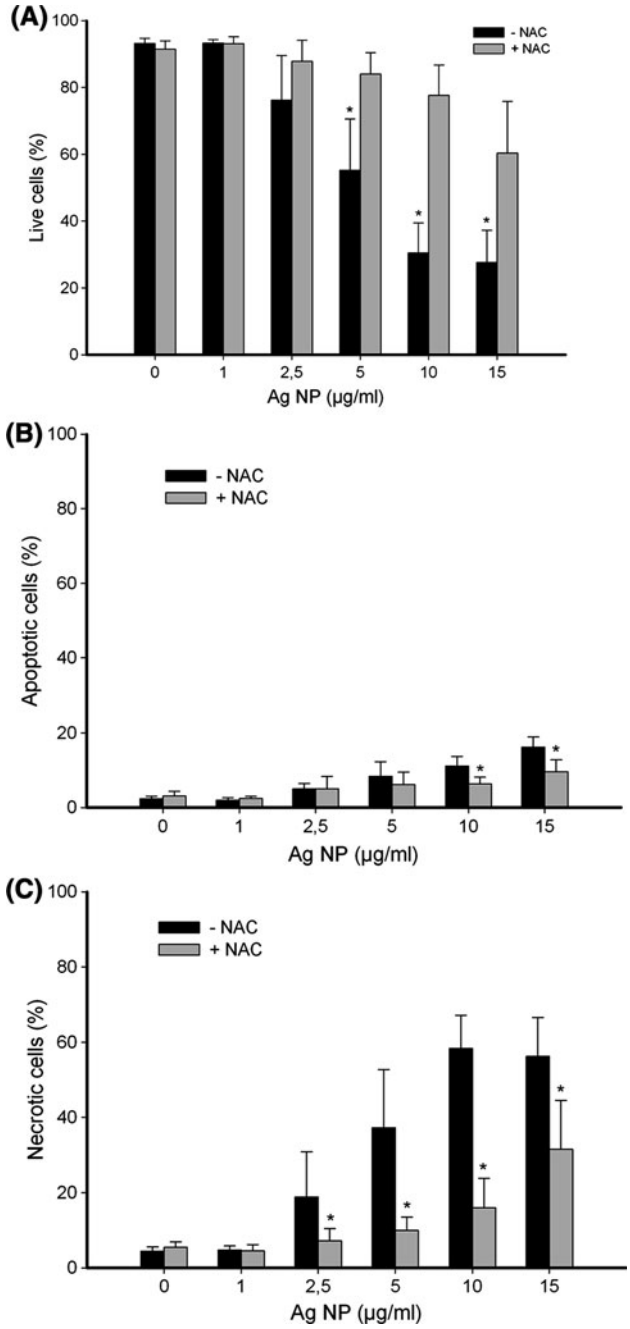

Fig. 3 Effect of Ag NPs on apoptosis and necrosis. Cells were pretreated for 1 h in media ± NAC (10 mM) followed by exposure to different concentrations of Ag NPs for 24 h. The annexin/PI assay was used to assess the percentage of **a** viable (annexin V−/PI−), **b** early apoptotic (annexin V+/PI−) and **c** late apoptotic/necrotic cells (annexin+/PI+). The data are expressed as mean ± SD of three independent experiments. *Asterisks* denote significant ($p < 0.05$) difference between samples ± NAC treatment at each Ag NP dose

Cellular DNA adducts

The experimental data suggest that Ag NPs are taken up by A549 cells resulting in oxidative stress and cell death. ROS have been shown to induce both direct and indirect damages to DNA. Using the ^{32}P postlabeling technique, we found a dose-dependent increase in the level of bulky DNA adducts after exposure to Ag NPs for 24 h (Fig. 5). Formation of bulky adducts was inhibited by 1-h pretreatment of the cells with NAC (10 mM).

Correlation analysis

Spearman's rank correlation coefficient (r_s) was calculated to investigate the possible correlation between ROS levels and mitochondrial damage, early apoptosis and DNA adducts, respectively. Strong correlations were observed when comparing ROS levels to mitochondrial damage ($r_s = -0.8810$; $p = 0.0039$), early apoptosis ($r_s = 0.8857$; $p = 0.0188$) or bulky DNA adducts ($r_s = 0.8810$, $p = 0.0039$).

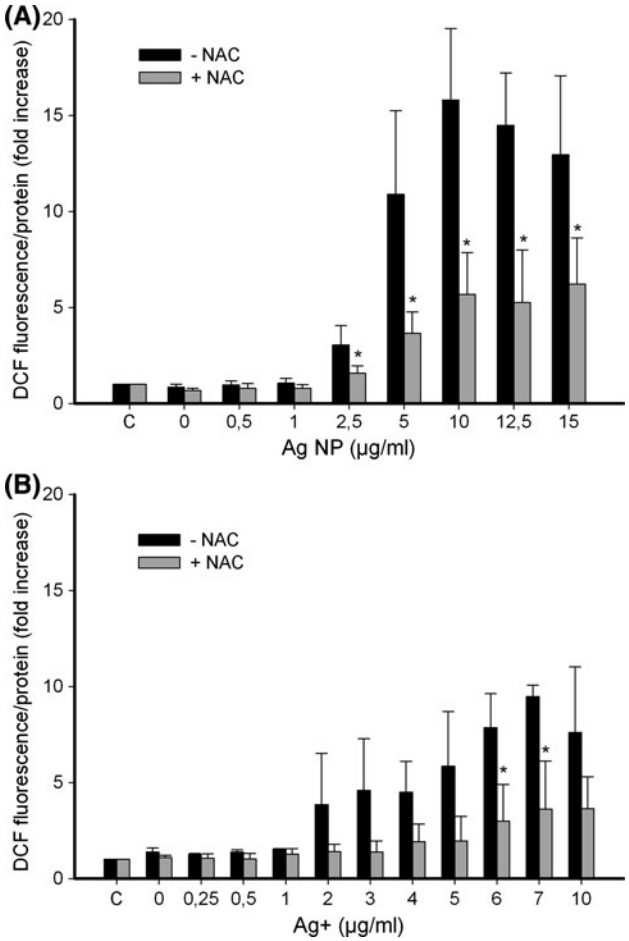

Fig. 4 Effect of Ag NPs and Ag+ on the cellular ROS levels. Cells were treated with NAC (10 mM, 1 h) and exposed to different concentrations of **a** Ag NPs or **b** Ag+ for 24 h. ROS and protein levels were measured by the fluorescence of DCF and fluorescamine, respectively. Data are reported as fold increase in DCF fluorescence/protein relative to controls. The data are expressed as mean ± SD of three independent experiments. *Asterisks* denote significant ($p < 0.05$) difference between samples ± NAC treatment at each Ag NP dose

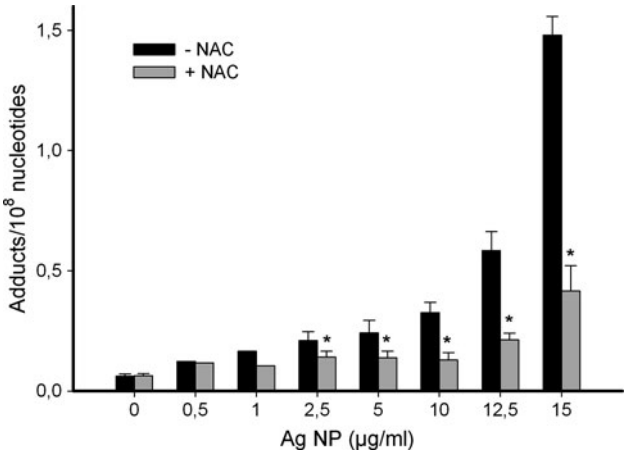

Fig. 5 Bulky DNA adducts after Ag NP exposure. Samples were pretreated for 1 h ± NAC (10 mM) and exposed to Ag NPs for 24 h. Bulky DNA adducts per 10^8 nucleotides were measured by ^{32}P postlabeling. *Asterisks* denote significant ($p < 0.05$) difference between samples ± NAC treatment at each Ag NP dose

Discussion

Size, shape and chemical composition have been deemed important properties when investigating NP-mediated toxicity (Auffan et al. 2009). The size, shape and stability of the NPs used in the present study were previously characterized by TEM, PW-XRD and DLS in both stock solution and RPMI media (Table 1). Our data suggest that when 1% FBS is added to the media, size and stability of the Ag NPs remain the same regardless of whether DMEM or RPMI is used as the exposure medium (unpublished data). However, the morphology and sizes of the NPs differ from the spherical shape, and 30–50 nm size reported by the manufacturer which emphasizes the importance of in-house characterization of NPs used in toxicological studies. Other properties of the Ag NP solution such as metal and endotoxin contamination which could greatly affect the cytotoxic effect were only found at very low levels in the present study, c.f. "Materials and Methods" and were regarded as insignificant.

The use of Ag NPs in consumer products and medical applications is rapidly expanding. As a consequence, industry workers, consumers and environment are anticipated to be increasingly exposed to Ag NPs. As one of the potential routes of human exposure is by inhalation of particles, an alveolar, epithelial, carcinoma cell line (A549) was used in the present study. An important issue in nanotoxicology is the uptake of NPs. Internalization of Ag NPs in human cell lines has been shown by TEM (AshaRani et al. 2009; Schrand et al. 2008). However, TEM is a time-consuming qualitative method for determining NP uptake. Accordingly, we used the light side scatter (granularity) of NP-exposed cells to demonstrate Ag NP uptake (Suzuki et al. 2007) which was verified by AAS measurements on cell lysates.

Internalization of NPs has been associated with decreased mitochondrial activity (Carlson et al. 2008; Xia et al. 2008). In the present study, Ag+ decreased mitochondrial activity more than Ag NPs with an approximately twofold difference in EC50 values which is in agreement with previous studies (Kim et al. 2009; Miura and Shinohara 2009). Importantly, NAC treatment of the cells significantly reduced the toxicity of both Ag NPs and Ag+ by up to 75%, suggesting the involvement of ROS. NAC primarily has a protective effect at high silver doses, indicating that the cellular antioxidant defense system is sufficient for protection against Ag NPs and Ag+ at low doses. NAC is a precursor for glutathione, and a number of studies have found increased ROS levels and depletion of GSH in cells

exposed to Ag NPs (Carlson et al. 2008; Hussain et al. 2005). Accordingly, protection of the cells against cytotoxicity could be due to NAC scavenging of ROS, but it could also be due to NAC binding of silver ions. It has been shown that silver ions have a high affinity for binding sulfhydryl groups and cysteine is a major binding site for Ag+ (Navarro et al. 2008). In the present study, Ag NPs appeared to induce higher increases in ROS than Ag+, indicating a particle-specific effect. e.g., ROS levels were increased by 15.8-fold and 7.6-fold of the control, respectively, at the same silver concentration (10 μg/ml). NAC treatment reduced the ROS levels, suggesting antioxidant scavenging as the mechanism of NAC-mediated cell survival. A strong correlation between ROS levels and mitochondrial activity could be calculated, further emphasizing the importance of ROS production in regard to Ag NP toxicity.

Increased ROS levels have previously been implicated in the signal transduction pathways leading to apoptosis (Ott et al. 2007; Ueda et al. 2002). It was also reported that apoptosis induced by Ag NPs was mediated by oxidative stress in fibroblast, muscle, colon and monocyte cell lines (Arora et al. 2008; Foldbjerg et al. 2009; Hsin et al. 2008). In this study, the main cause of cell death was detected as late apoptosis/necrosis, whereas less than 20% of the cells tested positive for early apoptosis. The involvement of ROS was indicated by a strong positive correlation between ROS production and early apoptosis. It should be noted that A549 cells have a constitutively high expression of heme oxygenase-1 which might render them less susceptible to ROS-induced cell death (Kweon et al. 2006).

ROS are considered to be one of the major sources of spontaneous damage to DNA. Oxidative attack on the DNA results in mutagenic modifications such as hydroxylation of adenine and guanine. In this study, we investigated the modification of DNA by the so-called bulky DNA adduct, which has been observed after exposure to chemicals and particles, e.g. PM2.5 (Sorensen et al. 2003). If not repaired, bulky DNA adducts could cause mutations leading to cancer (Smith et al. 2000). We found a dose-dependent increase in the level of bulky DNA adducts after exposure to Ag NPs for 24 h. Based upon migration pattern, the adducts were similar in the treated and untreated cells, suggesting that exposure to NPs induces higher levels of endogenously formed adducts (I-compounds). I-compounds are bulky covalent DNA modifications that can be detected and measured by ^{32}P-postlabeling. They were previously demonstrated to accumulate in an age-dependent, highly reproducible manner in tissue DNA of untreated animals in the absence of exogenous carcinogens and, therefore, appear to arise via the interaction of DNA with endogenous reactants formed in the course of metabolism, e.g. ROS (Randerath et al. 1990). The chemical identity of the bulky adducts has not been identified, but the inhibition of adduct formation by NAC suggests that ROS-mediated processes are involved. This is in correspondence with the strong positive correlation between ROS and bulky DNA adducts shown above. Bulky DNA adducts may lead to lesions that are expressed as micronuclei (Pavanello et al. 2008). Recently, the cytokinesis-blocked micronucleus assay was used to demonstrate an increase in micronuclei after exposure to Ag NPs which correlated with extensive and dose-dependent DNA damage as tested by the comet assay. Our unpublished results (Autrup) show that the type of adducts is independent of the type of NP. The mechanism of Ag NP-mediated DNA damage remains unclear although ROS appear to be implicated. Deposition of Ag NPs has been observed in the nucleus and the nucleolus thereby making the direct interaction between Ag NPs and DNA possible (AshaRani et al. 2009). However, the size of our Ag NPs is far larger than the diameter of the nuclear pore complexes (9–10 nm) thereby excluding this possibility.

The toxic effects of Ag NPs could theoretically be related to the release of free silver ions. However, two recent studies tested the content of free silver ions in Ag NP solutions and found low levels of Ag+ (0–1%). Furthermore, both studies concluded that the toxicity of Ag NP exposure could not be explained solely by the presence of Ag+ in the NP solution (Kim et al. 2009; Navarro et al. 2008). Our data suggest that Ag NPs induce higher levels of ROS than Ag+, and ICP data on the Ag NPs only show negligible levels of metal contaminants. Consequently, the question remains whether Ag NPs are intrinsically toxic or whether they act in a Trojan-horse like mode that enables uptake of the NPs and subsequent liberation of ions inside the cell (Limbach et al. 2007).

In conclusion, the present study showed that both Ag NPs and Ag+ could induce oxidative stress correlating with cyto- and genotoxicity. However, further studies are needed to elucidate the mechanism behind this process in order to facilitate the assessment of the risks and benefits of nano-sized silver compounds.

Acknowledgments The authors would like to thank Erik Baatrup, Institute of Biology, Aarhus University for conducting AAS measurements. The SUNANO project was granted by the Danish Strategic Research Council, NABIIT2006-06-0015.

Conflict of interest statement The authors declare that they have no conflict of interest.

References

Arora S, Jain J, Rajwade JM, Paknikar KM (2008) Cellular responses induced by silver nanoparticles: in vitro studies. Toxicol Lett 179(2):93–100

AshaRani PV, Low Kah MG, Hande MP, Valiyaveettil S (2009) Cytotoxicity and genotoxicity of silver nanoparticles in human cells. ACS Nano 3(2):279–290

Auffan M, Rose J, Bottero JY, Lowry GV, Jolivet JP, Wiesner MR (2009) Towards a definition of inorganic nanoparticles from an environmental, health and safety perspective. Nat Nanotechnol 4(10):634–641

Bak H, Autrup H, Thomsen BL, Tjonneland A, Overvad K, Vogel U, Raaschou-Nielsen O, Loft S (2006) Bulky DNA adducts as risk indicator of lung cancer in a Danish case-cohort study. Int J Cancer 118(7):1618–1622

Braydich-Stolle L, Hussain S, Schlager JJ, Hofmann MC (2005) In vitro cytotoxicity of nanoparticles in mammalian germline stem cells. Toxicol Sci 88(2):412–419

Carlson C, Hussain SM, Schrand AM, Braydich-Stolle LK, Hess KL, Jones RL, Schlager JJ (2008) Unique cellular interaction of silver nanoparticles: size-dependent generation of reactive oxygen species. J Phys Chem B 112(43):13608–13619

Foldbjerg R, Olesen P, Hougaard M, Dang DA, Hoffmann HJ, Autrup H (2009) PVP-coated silver nanoparticles and silver ions induce reactive oxygen species, apoptosis and necrosis in THP-1 monocytes. Toxicol Lett 190(2):156–162

Hsin YH, Chen CF, Huang S, Shih TS, Lai PS, Chueh PJ (2008) The apoptotic effect of nanosilver is mediated by a ROS- and JNK-dependent mechanism involving the mitochondrial pathway in NIH3T3 cells. Toxicol Lett 179(3):130–139

Hussain SM, Hess KL, Gearhart JM, Geiss KT, Schlager JJ (2005) In vitro toxicity of nanoparticles in BRL 3A rat liver cells. Toxicol In Vitro 19(7):975–983

Hussain SM, Javorina AK, Schrand AM, Duhart HM, Ali SF, Schlager JJ (2006) The interaction of manganese nanoparticles with PC-12 cells induces dopamine depletion. Toxicol Sci 92(2):456–463

Ip M, Lui SL, Poon VKM, Lung I, Burd A (2006) Antimicrobial activities of silver dressings: an in vitro comparison. J Med Microbiol 55(1):59–63

Kim S, Choi JE, Choi J, Chung KH, Park K, Yi J, Ryu DY (2009) Oxidative stress-dependent toxicity of silver nanoparticles in human hepatoma cells. Toxicol In Vitro 23(6):1076–1084

Kweon MH, Adhami VM, Lee JS, Mukhtar H (2006) Constitutive overexpression of Nrf2-dependent heme oxygenase-1 in A549 cells contributes to resistance to apoptosis induced by epigallocatechin 3-gallate. J Biol Chem 281(44):33761–33772

Limbach LK, Wick P, Manser P, Grass RN, Bruinink A, Stark WJ (2007) Exposure of engineered nanoparticles to human lung epithelial cells: influence of chemical composition and catalytic activity on oxidative stress. Environ Sci Technol 41(11):4158–4163

Lorenzen A, Kennedy SW (1993) A fluorescence-based protein assay for use with a microplate reader. Anal Biochem 214(1):346–348

Melaiye A, Sun Z, Hindi K, Milsted A, Ely D, Reneker DH, Tessier CA, Youngs WJ (2005) Silver(I)-imidazole cyclophane gem-diol complexes encapsulated by electrospun tecophilic nanofibers: formation of nanosilver particles and antimicrobial activity. J Am Chem Soc 127(7):2285–2291

Miura N, Shinohara Y (2009) Cytotoxic effect and apoptosis induction by silver nanoparticles in HeLa cells. Biochem Biophys Res Commun 390(3):733–737

Mosmann T (1983) Rapid colorimetric assay for cellular growth and survival: application to proliferation and cytotoxicity assays. J Immunol Methods 65(1–2):55–63

Navarro E, Piccapietra F, Wagner B, Marconi F, Kaegi R, Odzak N, Sigg L, Behra R (2008) Toxicity of silver nanoparticles to Chlamydomonas reinhardtii. Environ Sci Technol 42(23):8959–8964

Nielsen PS, de Peter N, Okkels H, Autrup H (1996) Environmental air pollution and DNA adducts in Copenhagen bus drivers—effect of GSTM1 and NAT2 genotypes on adduct levels. Carcinogenesis 17(5):1021–1027

Ott M, Gogvadze V, Orrenius S, Zhivotovsky B (2007) Mitochondria, oxidative stress and cell death. Apoptosis 12(5):913–922

Pavanello S, Kapka L, Siwinska E, Mielzynska D, Bolognesi C, Clonfero E (2008) Micronuclei related to anti-B[a]PDE-DNA adduct in peripheral blood lymphocytes of heavily polycyclic aromatic hydrocarbon-exposed nonsmoking coke-oven workers and controls. Cancer Epidemiol Biomarkers Prev 17(10):2795–2799

Randerath K, Li DH, Randerath E (1990) Age-related DNA modifications (I-compounds): modulation by physiological and pathological processes. Mutat Res 238(3):245–253

Schrand AM, Braydich-Stolle L, Schlager JJ, Dai L, Hussain SM (2008) Can silver nanoparticles be useful as potential biological labels? Nanotechnology 19:235104

Smith LE, Denissenko MF, Bennett WP, Li H, Amin S, Tang M, Pfeifer GP (2000) Targeting of lung cancer mutational hotspots by polycyclic aromatic hydrocarbons. J Natl Cancer Inst 92(10):803–811

Sorensen M, Autrup H, Moller P, Hertel O, Jensen SS, Vinzents P, Knudsen LE, Loft S (2003) Linking exposure to environmental pollutants with biological effects. Mutat Res 544(2–3):255–271

Suzuki H, Toyooka T, Ibuki Y (2007) Simple and easy method to evaluate uptake potential of nanoparticles in mammalian cells using a flow cytometric light scatter analysis. Environ Sci Technol 41(8):3018–3024

Ueda S, Masutani H, Nakamura H, Tanaka T, Ueno M, Yodoi J (2002) Redox control of cell death. Antioxid Redox Signal 4(3):405–414

van Engeland M, Ramaekers FC, Schutte B, Reutelingsperger CP (1996) A novel assay to measure loss of plasma membrane asymmetry during apoptosis of adherent cells in culture. Cytometry 24(2):131–139

Wijnhoven SWP, Peijnenburg WJGM, Herberts CA, Hagens WI, Oomen AG, Heugens EHW, Roszek B, Bisschops J, Gosens I, Van De Meent D, Dekkers S, De Jong WH, van Zijverden M, Sips ANJAM, Geertsma RE (2009) Nano-silver—a review of available data and knowledge gaps in human and environmental risk assessment. Nanotoxicology 3(2):109–138

Xia T, Kovochich M, Liong M, Madler L, Gilbert B, Shi H, Yeh JI, Zink JI, Nel AE (2008) Comparison of the mechanism of toxicity of zinc oxide and cerium oxide nanoparticles based on dissolution and oxidative stress properties. ACS Nano 2(10):2121–2134

Xia T, Li N, Nel AE (2009) Potential health impact of nanoparticles. Annu Rev Public Health 30(1):137–150